Electronic Supplementary Information

Covalent Organic Framework-Derived M1 Macrophage Mimic Nanozyme for Precise Tumor-Targeted Imaging and NIR-II Photothermal Catalytic Chemotherapy

Peng Gao [a‡], Kaixian Wang [a‡], Ruyue Wei [a], Xiaoying Shen [a], Wei Pan [a*], Na Li [a*], and Bo Tang [a,b*]

[a] College of Chemistry, Chemical Engineering and Materials Science, Key Laboratory of Molecular and Nano Probes, Ministry of Education, Collaborative Innovation Center of Functionalized Probes for Chemical Imaging in Universities of Shandong, Institute of Molecular and Nano Science, Shandong Normal University, Jinan 250014, P. R. China.

[b] Laoshan Laboratory, Qingdao 266237, P. R. China.

‡ These authors contributed equally to this work.

E-mail: panwei@sdnu.edu.cn, lina@sdnu.edu.cn, tangb@sdnu.edu.cn

1. Experimental Procedures

1.1 Chemicals: Tris(4-aminophenyl)amine (TAPA) and 2,5-Dimethoxybenzaldehyde (DMTP) were purchased from Energy Chemical (Shanghai, China). Acetic acid, acetonitrile and other reagents were purchased from Sinopharm Group Co. Ltd. (Hongkong, China). Mouse breast cancer cell line (4T1) was purchased from Jiangsu KeyGEN BioTECH Co., Ltd. 3-(4,5-dimethylthiazol-2-yl)-2,5-diphenyltetrazolium bromide (MTT) was purchased from Sigma Chemical Company. Confocal dish, glass bottom dishes were purchased from NEST Biotechnology Co. Ltd. (Wuxi, China). The ultrapure water of 18.2 MΩ cm was used throughout the experiments. Balb/C mice (6-8 weeks old, female, weight 18-21 g) were used in the experiment. All the other chemical reagents were of analytical grade and used without further purification.

1.2 Measurement and characterization: Absorption spectra were measured on a pharmaspec UV-1700 UV-visible spectrophotometer (Shimadzu, Japan). Fourier infrared spectrometer (Nicolet iS50 FT-IR) was used to characterize the infrared spectrum. Powder X-ray diffraction (XRD) pattern was obtained on a Rigaku SmartLab SE X-Ray Powder Diffractometer with Cu Kα line focused radiation (λ = 1.5405 Å). Transmission electron microscopy (TEM, HT7700, Japan) was carried out to characterize the morphology of the nanoparticles. Fluorescence spectra were obtained using a FLS-980 Edinburgh Fluorescence Spectrometer with a Xenon lamp. The absorbance was measured in a microplate reader (Synergy 2, Biotek, USA) for the MTT assay. Confocal fluorescence imaging studies were performed using a TCS SP8 confocal laser scanning microscope (Leica, Germany). All pH measurements were performed with a digital pH-meter (pH-3e, LeiCi, China).

1.3 The release of DOX in vitro: The synthesized D-PNC@M1m was dispersed in PBS buffer solution with pH=6.5 and 7.4, and stirred at 600 rpm at room temperature for different times (0, 1, 2, 3, 4, 8, 10, 12, 24, 48 h). The solution was collected and centrifuged at 15000 rpm to obtain the supernatant. The fluorescence intensity was then measured.

1.4 Cell culture: 4T1 cells were incubated in cell culture dishes with a diameter of 10 cm containing 1640 supplemented with 10 % fetal bovine serum (FBS), 1 % penicillin and streptomycin at 37 °C in a humidified atmosphere containing 5 % CO_2.

1.5 Cytotoxicity test: 4T1 cells were dispersed in 96-well plates and incubated for 24 h, then PNC@M1m and D-PNC@M1m in 1640 medium were incubated for 6 h. Then fresh culture medium was added and incubate for another 12 hours. Then the culture medium was removed from the

96-well, and 150 μL of MTT solution (0.5 mg/mL) was added. After incubated for 4 h, the MTT solution was removed, and 150 μL of DMSO was added. The absorbance at 490 nm was monitored by a microplate reader.

1.6 Detection of mitochondrial transmembrane potential (ΔΨm) : 4T1 cells were cultured in confocal dishes for 24 h and random divided into 5 groups (PBS, PBS+Laser, PNC@M1m+Laser, D-PNC@M1m, D-PNC@M1m+Laser). The cells were treated with PNC@M1m, D-PNC@M1m at a concentration of 90 μg/mL and incubated for 4 h. For all the laser irradiation groups, 1064 nm laser (1.0 W/cm^2) was utilized to irradiate the cells for 10 min. All the groups were further cultured for 12 hours. Finally, the cells were stained with Rhodamine 123 at 37 °C for 30 min and washed with PBS and analyzed with CLSM.

1.7 Establishment of tumor model: Animal experiments were reviewed and approved by the Ethics Committee of Shandong Normal University, Jinan, P. R. China (approval number AEECSDNU2023021). All animal experiments were conducted and obeyed the Principles of Laboratory Animal Care (People's Republic of China) and the Guidelines of the Animal Investigation Committee, Biology Institute of Shandong Academy of Science, China. Female Balb/c mice (6-8 weeks old, 18~21 g) were raised under normal circumstances of free access to water and goods. 1×10^7 4T1 cells in 100 μL of serum-free RPMI 1640 medium were injected subcutaneously into the right axillary region of the Balb/c mice. The mice were used into subsequent therapy experiments until the tumor volume had reached approximately 75-100 mm^3.

1.8 In vivo antitumor experiment: The 4T1 tumor bearing Balb/c mice were randomly divided into 6 groups (PBS, PBS+Laser, PNC@M1m, PNC@M1m+Laser, ID-PNC@M1m, ID-PNC@M1m+Laser). The nanoparticle (10 mg/kg) was administered to each mouse by intravenous injection. For all the laser irradiation groups, 1064 nm laser (1.0 W/cm^2) was utilized to irradiate the tumor site for 10 min. After that, the tumor growth and body weight change situations of the Balb/c mice were observed and recorded within 14 days.

1.9 Statistical Analysis: All data were reported as the mean ± s.d.; n = 3 for all in vitro. n = 5 for in vivo anticancer studies. The difference between two groups was analyzed by independent sample t-test. The statistical significance was indicated as $p < 0.05$, and ex-pressed as *$p < 0.05$, **$p < 0.01$, ***$p < 0.001$, ****$p < 0.0001$.

2. Supplementary Figures

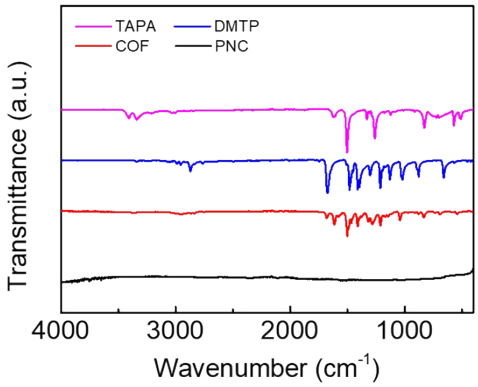

Figure S1. The FT-IR spectra of COF monomers, COF and PNC.

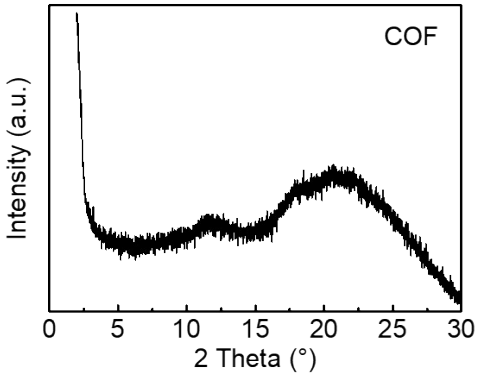

Figure S2. The PXRD pattern of COF.

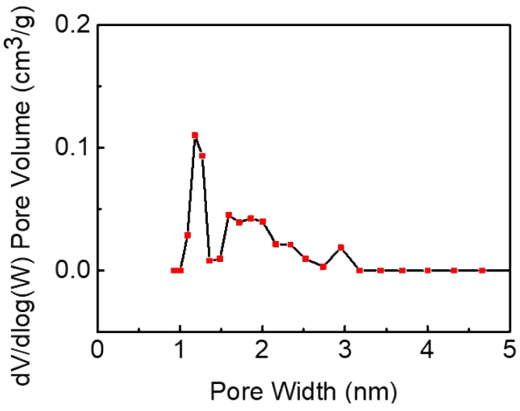

Figure S3. The pore width distribution of COF.

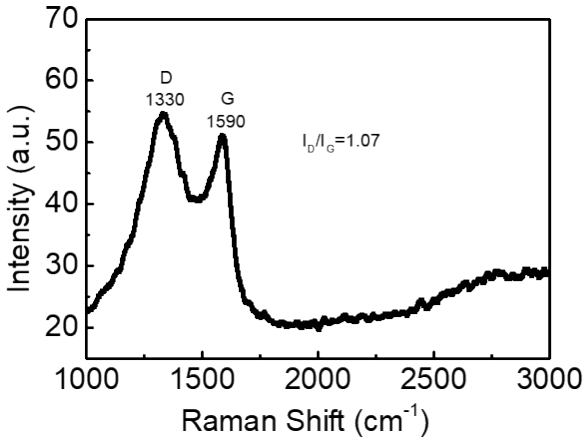

Figure S4. Raman spectrum of PNC.

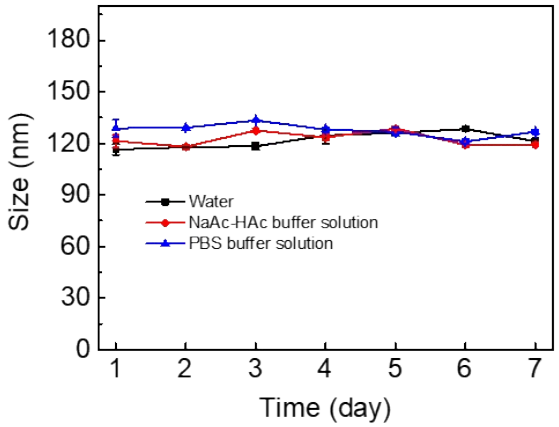

Figure S5. DLS size distribution of ID-PNC@M1m during incubation in different solutions for a week.

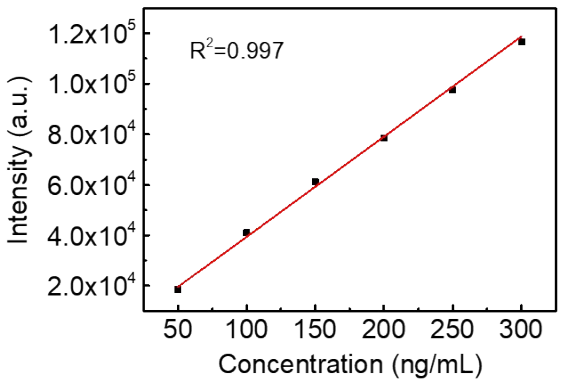

Figure S6. Fluorescence standard curve of IR808 solution.

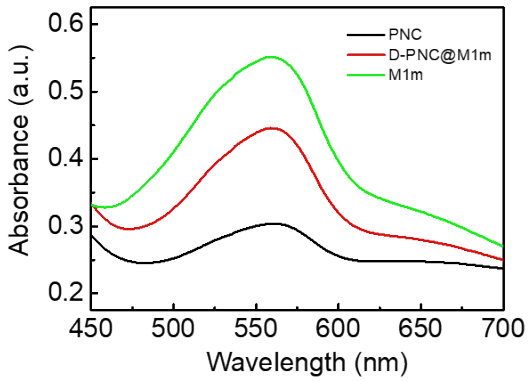

Figure S7. The UV-Vis absorbance of different materials after treatment with the BCA assay kit.

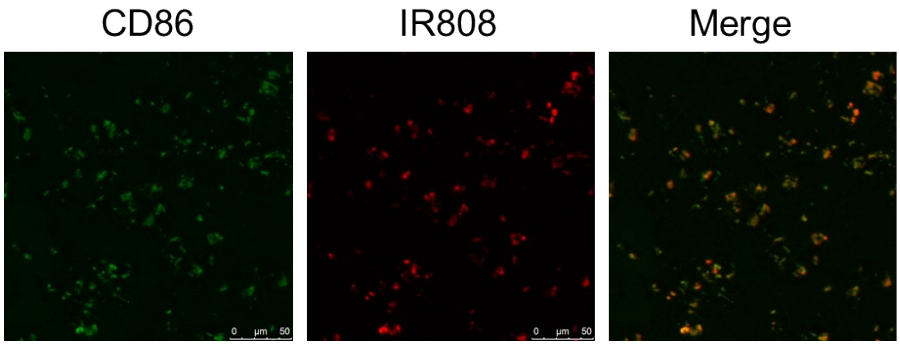

Figure S8. Immunofluorescence imaging of CD86 in ID-PNC@M1m.

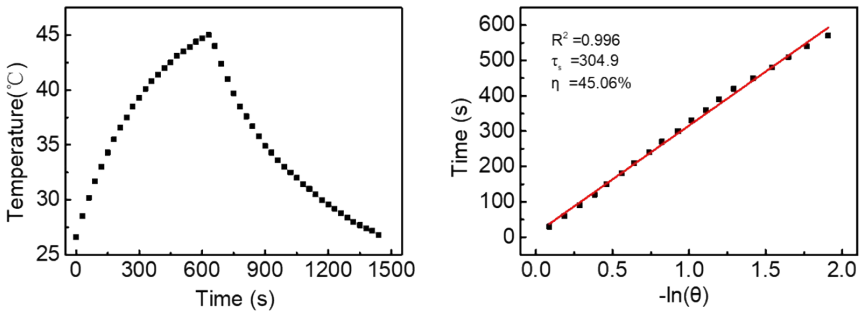

Figure S9. Left: Temperature change of PNC solution under laser switch-on and switch-off treatment. Right: calculation of the photothermal conversion effect of PNC.

Figure S10. The photograph of TMB treated with H_2O_2 (left) and H_2O_2+PNC (right).

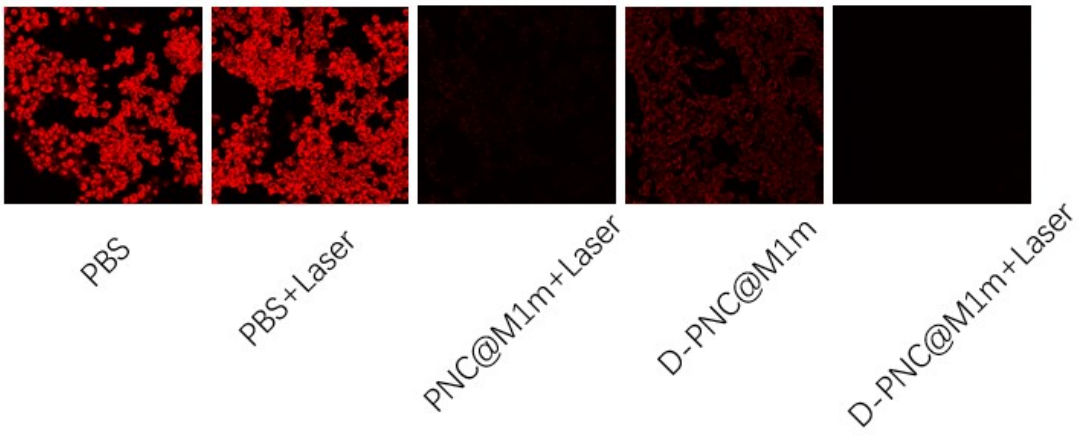

Figure S11. Confocal images of 4T1 cells with different treatments using Rhodamine123 as the membrane potential indicator.

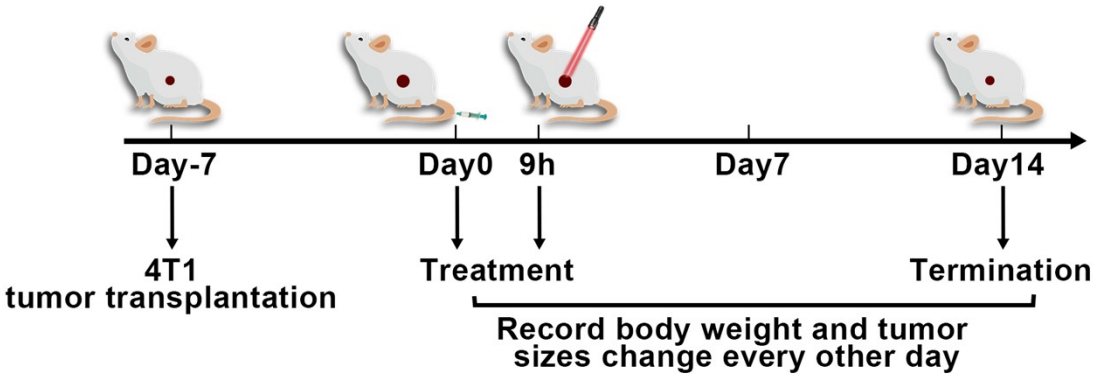

Figure S12. Diagrammatic instruction of the therapeutic process.

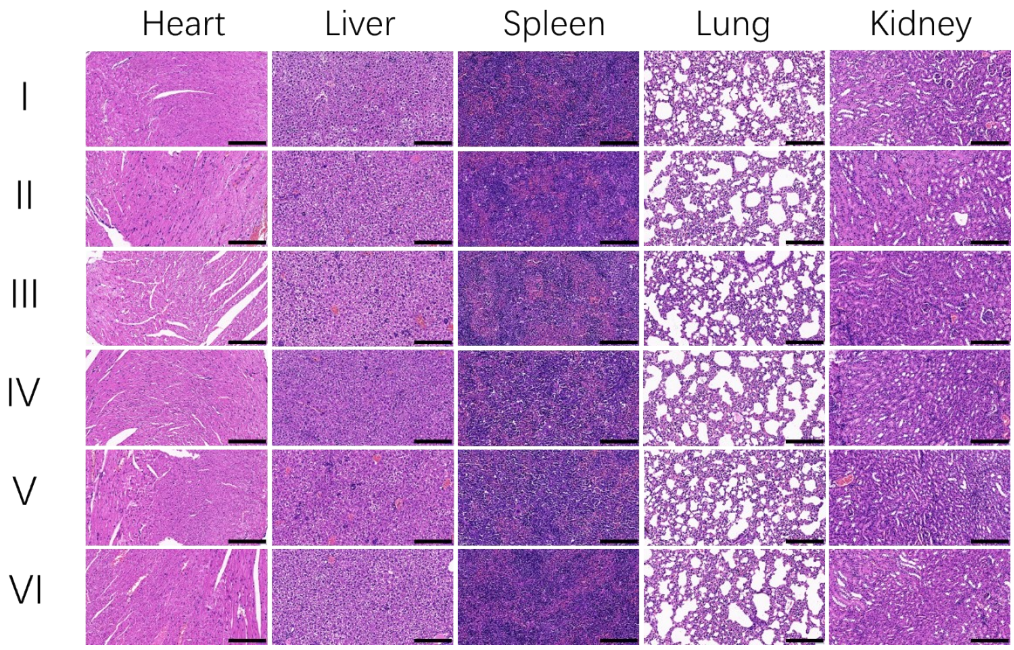

Figure S13. The H&E staining of the slices of the main organ of mice from different groups. Scale bars are 200 μm. (I) PBS, (II) PBS+Laser (III) PNC@M1m (IV) PNC@M1m+Laser (V) ID-PNC@M1m and (VI) ID-PNC@M1m+Laser.

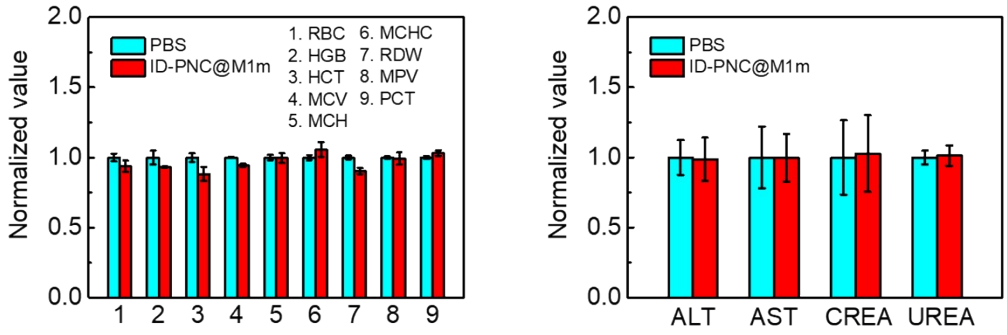

Figure S14. The hematological and histological analysis of mice in PBS and ID-PNC@M1m group.